PHOTOPRODUCTION OF π^+ MESONS FROM PROTONS AT E_γ = 230 MeV AND DETERMINATION OF THE $\gamma\pi\rho$ COUPLING CONSTANT

Yu. M. ALEKSANDROV, V. F. GRUSHIN, V. A. ZAPEVALOV, and E. M. LEĬKIN

P. N. Lebedev Physical Institute, Academy of Sciences, U.S.S.R.

Submitted to JETP editor January 29, 1965

J. Exptl. Theoret. Phys. (U.S.S.R.) 49, 54-65 (July, 1965)

The differential cross section for photoproduction of π^+ mesons from protons at an energy E_γ = 230 MeV has been measured for center-of-mass angles of 0, 38, 82, 90, 116, 138, 146, and 180°. A magnetic spectrometer and a meson-stopping detector were used to identify mesons from momentum and range. Stopped π^+ mesons were detected by means of the $\pi \to \mu$ decay. The statistical accuracy of the results is ±(3—4)% on the average. From comparison of the experimental data with theoretical calculations based on dispersion relations, we have estimated the value of the $\gamma\pi\rho$ coupling constant, $\Lambda_{\gamma\pi\rho} = (0.63 \pm 0.11)ef$.

THE study of photoproduction of π mesons from nucleons enables us to obtain information on the processes occurring in the meson-nucleon system. The principal features of the experimental results in the energy region near the photoproduction threshold and in the region of the first resonance are described by dispersion theory. Further investigation of the weaker effects appearing in this phenomenon provides the possibility of incorporating them in the theory and of obtaining accurate experimental data. One of these effects which has been frequently discussed recently is the resonance interaction of π mesons (the ρ and ω mesons). The isotopic-spin structure of the photoproduction amplitudes allows contributions of both the $\gamma\pi\rho$ and $\gamma\pi\omega$ interactions to appear in the case of π^0-meson photoproduction, and only the first of these interactions in photoproduction of π^+ mesons. The differential cross sections at large meson angles turn out to be the most sensitive to this effect.

Comparison of the experimental results with theoretical calculations taking into account the contribution of these effects to the photoproduction amplitudes affords a possibility of obtaining quantitative estimates of the $\Lambda_{\gamma\pi\rho}$ and $\Lambda_{\gamma\pi\omega}$ coupling constants.

The contemporary level of experimental technique in principle permits establishment of the constant Λ with an uncertainty matching the degree of approximation of the theory. The present work is devoted to measurement of the angular distribution of π^+ mesons produced in the reaction $\gamma + p \to \pi^+ + n$ at a photon energy E_γ = 230 MeV. The results of the few experiments performed at this energy up to the beginning of the present work [1,2] were rather contradictory and did not have the necessary degree of accuracy.

1. DESCRIPTION OF METHOD AND EXPERIMENTAL APPARATUS

The experiment was performed in the bremsstrahlung beam of the 265-MeV synchrotron at the Physics Institute of the Academy of Sciences.

Determination of the photon energy was based on knowledge of the energy and angle of the π meson and the unique kinematics of the reaction. π^+ mesons of a given energy were detected by a method involving identification of the particles from their momentum and range in matter. This was accomplished by a magnetic spectrometer and a detector of π^+-meson stoppings—a scintillation counter telescope containing a copper absorber of a definite thickness. π^+ mesons stopped in one of the counters were reliably identified from the $\pi \to \mu$ decay, which occurs with the characteristic time $\tau_\pi = 2.55 \times 10^{-8}$ sec. Momentum analysis of the particles was performed in the measurements at 0 and 180°; at the remaining angles only the stopping detector was used.

Figure 1 shows schematically the arrangement of the apparatus for the 180° measurements. In the 0° measurements the magnet and the target changed places.

The work was performed with one of two spatially separated bremsstrahlung beams corresponding to two targets located at different points of the electron orbit of the accelerator. [3] This photon

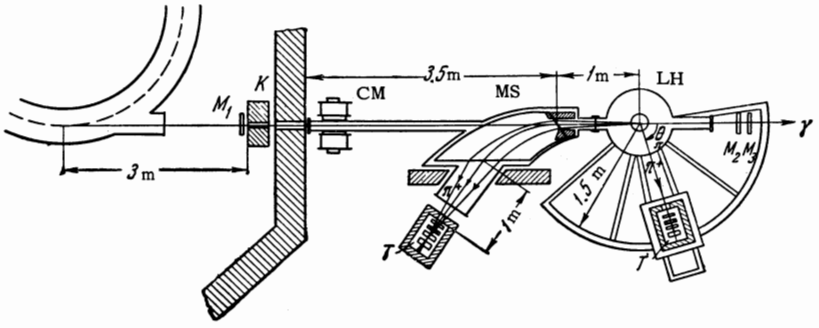

FIG. 1. Schematic drawing of the experimental apparatus: K – lead collimators, the first of which is of conical shape, CM – clearing magnet, MS – magnetic spectrometer, LH – liquid hydrogen target, M_1, M_2, M_3 – monitor ionization chambers, T – scintillation counter telescope.

beam after collimation had a cross section at the target location of 2.8 cm diameter (for the 0° measurements the diameter was 2.0 cm). After the lead collimators was placed a clearing magnet whose field was ~ 3500 G.

The entire region in the path of the photon beam from the clearing magnet to the target, and also in the path of the π^+ mesons through the magnetic spectrometer, was evacuated by means of a single system of fore pumps. This system included the vacuum pipe and vacuum chamber of the magnetic spectrometer and was separated from the high-vacuum region of the target by a copper foil of thickness 0.05 mm. The side wall of the spectrometer chamber consisted of vacuum rubber 6 mm thick, stretched between the pole tips and pressure-sealed to them along their perimeters; the top and bottom of this chamber were formed by the pole tips themselves. The rubber wall also sealed the flanged joints of the chamber to the vacuum pipe along the photon beam and to the π^+-meson tube to the telescope.

The experimental setup included a vacuum-insulated liquid-hydrogen target (Fig. 2) with liquid-nitrogen cooling. [4] The cylindrical appendix of the target with its flange was turned in one piece from a duraluminum bar. Its diameter was 80 mm, its height 90 mm, and the wall thickness traversed by the x-ray beam was 0.065 mm. The appendix was joined to the hydrogen reservoir by an indium gasket. The total volume of the hydrogen reservoir and the appendix amounted to 10.6 liters. One filling of the target with a liquid mixture of ortho and para hydrogen (3:1) provided continuous measurements for a period of 120 hours. The liquid hydrogen level was controlled by two capacitance probes. The secondary particles emerged through 10 × 15 cm^2 windows in the external jacket of the target, which were covered with stainless steel foil 0.1 mm thick.

To measure the angular distribution between 0 and 180°, we built a special frame which could be moved along a circular track of radius 1.5 m around an axis passing through the center of the

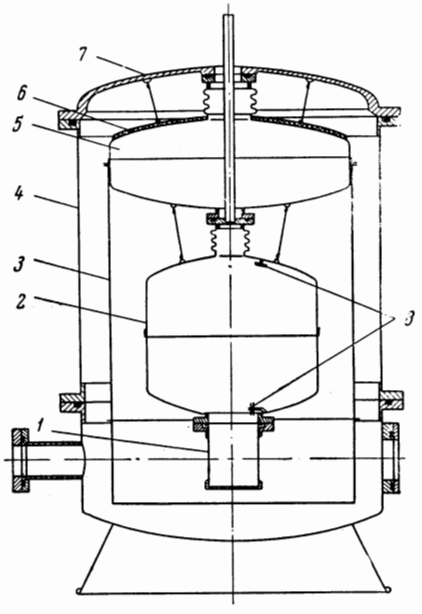

FIG. 2. Design of the liquid hydrogen target (vertical section): 1 – appendix, 2 – hydrogen reservoir, 3 – heat shield, 4 – external jacket, 5 – liquid-nitrogen reservoir, 6 – activated charcoal, 7 – top plate, 8 – capacitive probe for hydrogen level.

massive support for the target. The axis of the appendix coincided with the axis of rotation of the frame. On the frame was mounted a cart which could be moved radially. On the cart was located the telescope of scintillation counters, surrounded by lead shielding in the front wall of which there was a circular opening 4.5 cm in diameter constituting the entrance aperture of the telescope.

Monitoring of the primary x-ray beam was accomplished by means of three thin-walled differential ionization chambers. The basis of the electronic part of the monitors was a circuit working on the principle of recharging the grid capacitance of a blocking-oscillator tube. [5] A check of the relative readings of the monitors showed that the stability of the readings was within 0.5%. The absolute reading of the monitors throughout the whole experiment was determined from the readings of a quantameter [6,7] which was periodi-

cally placed in the beam behind the double monitors M_2, M_3.

The counters of the telescope contained plastic scintillators (a solid solution of 3% p-terphenyl in polystyrene with addition of a wavelength shifter) in the form of discs joined to the photomultiplier cathode by conical Plexiglas light pipes. [8] The scintillator diameters were 100 mm, and the thickness 10 mm for counters 1 and 2, 20 mm for counter 3, and 35 mm for counter 4. Counters 1, 2, and 4 used standard fast photomultipliers of type FÉU-36 operating directly into a long, terminated RK-2 cable. However, these photomultipliers turned out to be unsuitable for use in the stopping counter (No. 3) because of the presence of afterpulses which simulated $\pi \rightarrow \mu$ decay events. For this reason counter 3 utilized a modified FÉU-36 in which decoupling capacitors were introduced inside the bulb in the circuits of the last two dynodes to suppress afterpulses. [9] Shielding of the photomultipliers from the stray magnetic field was provided by a common shield of several layers of soft iron.

As we have already noted, in the 0° and 180° measurements the positively charged secondary particles were deflected and simultaneously momentum-analyzed by a magnetic spectrometer. The pole tips had a sector shape and produced a magnetic field with double-focusing properties. [10,11] For a useful magnet gap of 6 cm and a current of 30 A in the coils the field in the central region reached 8000 G. Because of the strong nonuniformity of the spectrometer field, the trajectories of the charged particles passing through the magnetic field region were determined by the hot-wire method. [12] This trajectory tracing was carried out from different points of the target and to a rather large distance from the magnetic field region. We determined the projections of the appropriate trajectories on the horizontal and vertical planes before and after the magnetic spectrometer.

The hot-wire tracing utilized a copper wire 0.1 mm in diameter carrying a current of 0.75 A. The current was maintained constant within 0.1%. The wire tension was provided by balanced suspension of a weight from one of its ends and was determined with an accuracy of 0.2%. The momentum values and trajectory directions in space obtained from averaging the results of repeated tracings had an error of less than 1%. The magnet dispersion found from these data at the location of the telescope entrance aperture was 1.37 ± 0.05 (MeV/c) cm^{-1} and 1.44 ± 0.07 (MeV/c) cm^{-1} respectively for 0° and 180°. For a given entrance aperture of the telescope we determined the entrance aperture of the magnetic spectrometer, which allowed us to find the solid angle of the entire apparatus: 1.15×10^{-3} sr (for 0°) and 1.25×10^{-3} sr (for 180°).

The 0° measurements were characterized by heavy loading of the counters by positrons of the same momentum as the π^+ mesons. Under our conditions, when the total amount of material in the photon beam was 0.014 radiation length (of this 0.009 radiation length was in the liquid hydrogen), 10^5 positrons passed through the telescope for each π^+ meson stopping in it. This fact required increased reliability of π^+-meson identification. Therefore we specially developed two versions of the detection apparatus, [13] one of which was intended for measurements under conditions of high positron background, and the other for measurements with ordinary background.

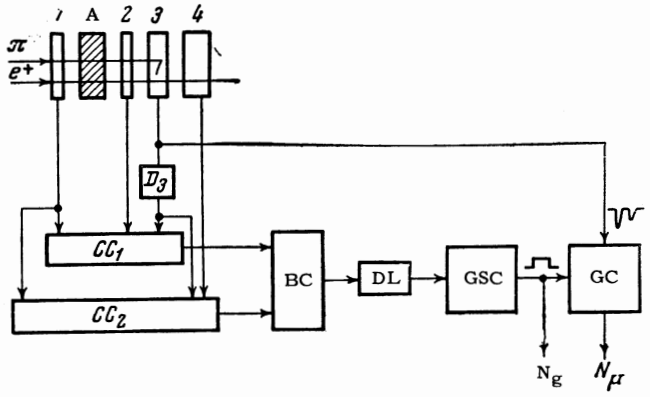

FIG. 3. Block diagram of detecting apparatus intended for operation in conditions of large positron background: 1–4 – scintillation counters, A – bremsstrahlung absorber, CC_1 and CC_2 – triple-coincidence circuits, BC – blocking circuit, DL – variable delay line, GSC – gate-shaping circuit, GC – gate circuit for μ-meson pulse, D_3 – fast amplitude discriminator, N_g – number of gate pulses counted, N_μ – number of delayed coincidences.

Figure 3 shows a block diagram of the first version of the apparatus. The basis of this version (and also of the second version) is the detection of delayed coincidences between a gate pulse produced by a π^+ meson and the pulse from decay of the μ^+ meson. Use of a long gate (1.2×10^{-7} sec) permits avoiding additional losses in counting decay events, and the uncertainty in the gate length introduces practically no error in the detection efficiency. However, because of the low resolving time of the delayed-coincidence circuit, we took measures to reduce the number of times the gate was triggered by positrons.

The presence of an anticoincidence counter

(No. 4) in the telescope allows us to utilize the difference in ranges of π^+ mesons and positrons of the same momentum. For the case when a π^+ meson stops in counter No. 3, a pulse occurs at the output of the triple-coincidence circuit CC_1 which is transmitted to the gate-shaping circuit GSC. A pulse from the similar coincidence circuit CC_2 arises only when a positron hits the telescope; this pulse blocks passage of the pulse from CC_1 to GSC. Since this blocking of the positrons cannot be complete because of bremsstrahlung in counter No. 3, further discrimination against positrons was performed in counter channels 2 and 3 on the basis of the energy dissipated by the positrons. In counter channel No. 2 this was achieved by reducing the photomultiplier gain so as to reduce the positron counting rate with practically no loss in π^+-meson counting rate, which is illustrated in Fig. 4. In counter channel No. 3, a fast amplitude discriminator D_3 was introduced whose operation threshold corresponded to an energy loss by the fast positron 1.5 times greater than the probable value. In Fig. 5, curve 1 is a calibration curve of the discriminator as a function of the energy dissipated and curve 2 shows the number of delayed coincidences as a function of the discriminator level.

In the second version of the apparatus, counter No. 4 is absent and correspondingly the circuits CC_2 and DL. Instead of the triple-coincidence circuit, a double-coincidence circuit for counters 1 and 2 was used, and the pulse from counter 3 was fed only to the gate circuit.

2. ANALYSIS OF RESULTS

The measurement procedure consisted of taking a delayed-coincidence curve, i.e., the number of counts N_μ as a function of the delay in the gating channel. Figure 6 shows such a curve taken for $\theta_{c.m.} = 90°$, which, after a certain delay, becomes a $\pi \rightarrow \mu$ decay curve.

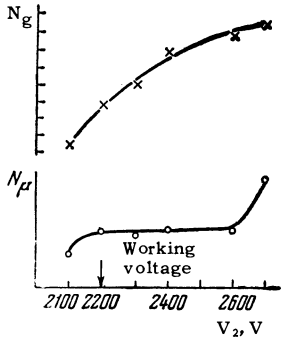

FIG. 4. Gate counting rate N_g and delayed coincidence counting rate N_μ, as a function of photomultiplier voltage (counter No. 2).

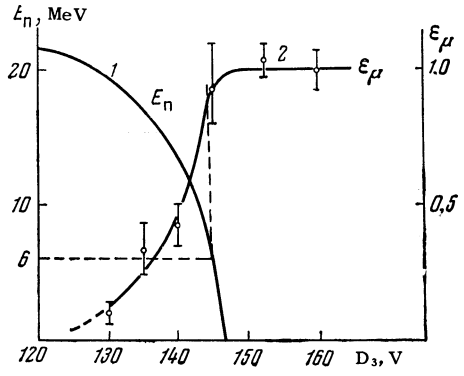

FIG. 5. The experimental dependence of the efficiency of detection of a μ-meson pulse on the level of the discriminator D_3, obtained in a measurement at one of the photoproduction angles – curve 2. Relation between the energy dissipated in counter 3 and the discriminator level, computed on the basis of curve 2 – curve 1. The threshold energy deposition of 6 MeV (1.5 times the probable ionization loss of fast positrons) corresponds to $\epsilon_\mu = 0.95$.

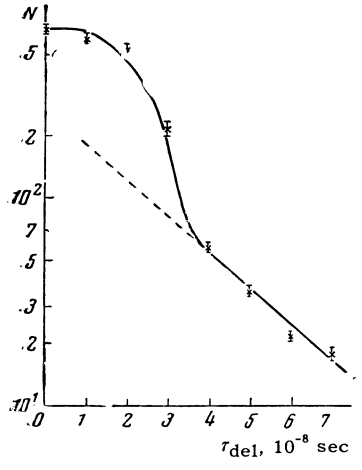

FIG. 6. Delayed coincidence curve, measured at $\theta_{c.m.} = 90°$ and plotted on a semilogarithmic scale. The straight line corresponds to a mean life of $\tau_\pi = 2.55 \times 10^{-8}$ sec.

Measurements were made at eight meson angles: 0, 38, 82, 90, 116, 138, 146, and 180°.

The energy resolution of the equipment in measurements with the telescope without the magnetic spectrometer is determined by the kinematic relation between E_π, θ_π, and E_γ. For a constant telescope entrance aperture ($\Delta\theta_\pi$ = const) and a constant stopping-counter thickness ($\Delta E_\pi \approx$ const), the width of the photon energy interval ΔE_γ producing detected events is a function of θ_π. This can be seen from Fig. 7, which shows the kinematic relation for the reaction studied. When the magnetic spectrometer is used, the energy resolution of the apparatus is due to the dispersion of the magnet and the size of the telescope entrance aperture.

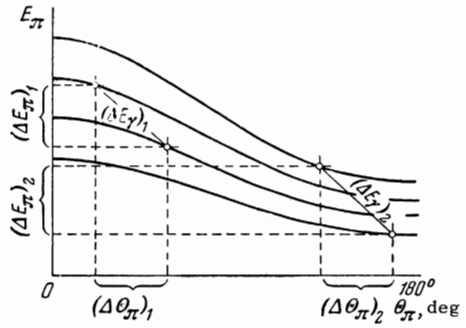

FIG. 7. Schematic illustration of the kinematic relation $F(E_\pi, E_\gamma, \theta_\pi) = 0$ for the reaction $\gamma + p \to \pi^+ + n$ for $(\Delta E_\pi)_1 = (\Delta E_\pi)_2$, $(\Delta\theta_\pi)_1 = (\Delta\theta_\pi)_2$, and $(\Delta E_\gamma)_2 > (\Delta E_\gamma)_1$.

The series of values of N_μ measured for different delays (for a standard monitor reading) were subjected to verification of their statistical compatibility, after which mean values $\overline{N}_\mu$ were determined for delays corresponding to the $\pi \to \mu$ decay curve. An accidental coincidence background was observed in the measurements at 0 and 180°, but was practically absent for the other angles. After separation of the background, the values of $\overline{N}_\mu$ were converted to the number of π^+ mesons stopping in the telescope $\overline{N}_\pi$. The determination of the conversion coefficients took into account the shape of the rise of the instantaneous coincidence curve, which was obtained in an experiment with a beam of monoenergetic positrons. From the values of $\overline{N}_\pi$ found from the experimental results for several delays, we determined a weighted mean value $\widetilde{N}_\pi$. The empty-target contribution to this value was negligibly small.

The values of $\widetilde{N}_\pi(\theta_\pi)$ are related to the differential cross sections for photoproduction of π^+ mesons for each of the measured angles by the formula

$$\widetilde{N}_\pi(\theta_\pi) = \varepsilon x \int\int N_\gamma(E_\gamma)\,\Omega(\mathbf{r}, E_\gamma, \theta_\pi)\frac{d\sigma}{d\Omega_{\text{c.m.}}}(E_\gamma, \theta_\pi)\frac{d\Omega_{\text{c.m.}}}{d\Omega_{\text{lab}}} \times \frac{dn}{dv}\rho(\mathbf{r})\,\eta(E_\gamma, \theta_\pi)\,\delta(E_\gamma, \theta_\pi)F(E_\gamma, \theta_\pi)\,dv\,dE_\gamma, \qquad (1)$$

where ϵ is the counting efficiency for decay μ mesons, x is the effective thickness of the target in cm, $N_\gamma(E_\gamma)$ is the bremsstrahlung spectrum, $\Omega(\mathbf{r}, E_\gamma, \theta_\pi)$ is the efficiency function of the apparatus for a point target, $d\Omega_{\text{c.m.}}/d\Omega_{\text{lab}}$ is the solid angle transformation from the center-of-mass to the laboratory system, dn/dv is the density of nuclei in the target in cm^{-3}, $\rho(\mathbf{r})$ is the relative distribution of the photon beam intensity, η, δ, and F are corrections for decay in flight, nuclear absorption, and multiple Coulomb scattering of π^+ mesons, and $d\sigma/d\Omega_{\text{c.m.}}(E_\gamma, \theta_\pi)$ is the differential cross section in the center-of-mass system of the colliding particles.

The efficiency functions, averaged over the target volume,

$$\widetilde{\Omega}(E_\gamma, \theta_\pi) = \int \Omega(\mathbf{r}, E_\gamma, \theta_\pi)\,\rho(\mathbf{r})\,dv$$

were calculated on the FIAN electronic computer on the basis of the experimental geometry, the kinematics of the reaction, the energy loss of π^+ mesons in the target and in the telescope,[1)] and the dispersion of the magnetic spectrometer. The efficiency functions calculated for 90° and 180° are shown for illustration in Fig. 8.

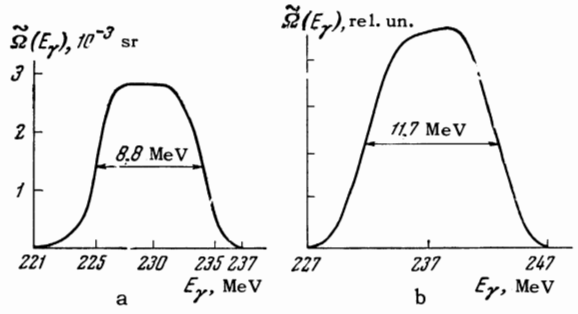

FIG. 8. Efficiency function $\Omega(E_\gamma)$, calculated for the cases: a – $\theta_{\text{lab}} = 74°$ ($\theta_{\text{c.m.}} = 90°$), b – $\theta_{\text{c.m.}} = 180°$ (in relative units).

The spectrum $N_\gamma(E_\gamma)$ was computed on the basis of the Schiff integrated-over-angle spectrum, taking into account the duration of the x-ray burst.

The corrections described above, within the limits of the energy resolution of the equipment, are weakly varying functions of the energy E_γ, and were therefore computed for an average energy $\overline{E}_\gamma$ ($\overline{\eta}$, $\overline{\delta}$, $\overline{F}$), taking into account the slowing down of the π^+ mesons in the telescope.

Table I lists the main results of the experiment and a number of quantities entering into formula (1). The differential cross-section value for 180°, obtained from the experimental data for E_γ = 237.5 MeV, was converted to E_γ = 230 MeV on the basis of the theoretical energy dependence of the cross section for this angle. The errors indicated in the table are statistical, including that for $\theta_\pi = 0°$, where the error listed reflects the presence of the large accidental-coincidence background. The remaining results have a statistical accuracy on the average of ±(3—4)%.

[1)] In this calculation we used the mean ionization potentials for the various materials from the work of Sternheimer,[14] Barkas and Von Friesen,[15] and Sternheimer.[16]

Table I

θ_{cm}, deg	$\bar{E}_\gamma$, MeV	$\frac{\Delta E_\gamma}{\bar{E}_\gamma}$, %	$\bar{\eta}$	$\bar{\delta}$	$\bar{F}$	$\bar{\eta}\,\bar{\delta}\,\bar{F}$	$\int N_\gamma \tilde{\Omega} dE_\gamma \cdot 10^{-8}$ photons-sr	ε	$\frac{d\Omega_{lab}}{d\Omega_{c.m.}}$	$\tilde{N}_\pi$	$\frac{d\sigma}{d\Omega_{c.m.}}$, 10^{-33} cm^2
0	232.1	1.2	0.660	0.807	0.965	0.515	1.49	0.51	0.585	5.7±2.5	7.35±3.25
38	231.5	2.6	0.885	0.789	0.900	0.629	21.2	0.72	0.636	85.8±4.0	7.15±0.34
82	230.1	3.5	0.876	0.881	0.938	0.724	34.2	0.95	0.845	163.5±4.9	11.30±0.33
90	228.9	3.8	0.870	0.902	0.944	0.738	37.5	0.95	0.907	177.7±5.0	12.10±0.31
116	230.1	5.2	0.849	0.961	0.971	0.791	49.6	0.95	1.177	232.0±8.1	12.75±0.45
138	229.0	7.0	0.838	0.978	0.980	0.802	66.6	0.95	1.471	263.8±8.2	14.64±0.44
146	230.0	7.4	0.822	0.983	0.982	0.792	63.7	0.95	1.580	214.7±5.3	13.66±0.33
180	237.5	5.0	0.572	0.999	0.989	0.565	8.25	0.95	1.854	20.9±1.0	14.35±0.69
	(230)										(13.65±0.66)

The absolute cross sections may contain systematic errors, the main contribution to which is from the uncertainty in the quantameter constant (± 5%). In addition, introduction of the corrections $\bar{\eta}$, $\bar{\delta}$, and $\bar{F}$ involves an error of ± 1.5%. The uncertainty in converting $\bar{N}_\mu$ to $\bar{N}_\pi$ amounts to ± 2%; the error due to inaccurate values of the density of nuclei in the target, the geometrical constants of the apparatus, and the maximum energy of the bremsstrahlung spectrum amounts to ± 2%. In total, the mean-square systematic error of the differential cross section values listed does not exceed ± 6%.

3. DISCUSSION OF RESULTS

Figure 9 shows the results of the present work on measurement of the angular distribution of π^+ mesons for E_γ = 230 MeV, together with the data of Tollestrup et al., [1] Walker et al., [2] and Adamovich et al., [17] obtained at different times and by different methods. It is evident that, except for the data of Tollestrup et al. [1] in the forward

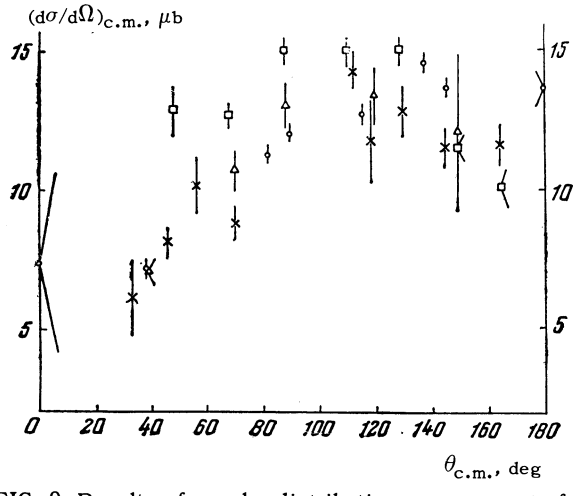

FIG. 9. Results of angular distribution measurements for the process $\gamma + p \to \pi^+ + n$ for E_γ = 230 MeV, obtained by different authors: □ – Tollestrup et al.[1], Δ – Walker et al.[2], × – Adamovich et al.[17], o – present work.

hemisphere, the remaining results are consistent; however, there are some differences in the large-angle region.

Comparison of the results obtained by us with a calculation based on dispersion relations [17] for different values of the $\gamma\pi\rho$ coupling constant $\Lambda_{\gamma\pi\rho}$ (see Fig. 10a) allows us to obtain an estimate of the value of this constant. For this purpose we plotted the likelihood function

$$L(\Lambda) = \prod_{i=1}^{8} p(\theta_\pi{}^i, \Lambda),$$

where $p(\theta_\pi^i, \Lambda)$ is the probability that the experimental result for θ_π^i is comparable with the theoretical result with a certain value of Λ. From the position of the peak and the shape of the L(Λ) curve we obtained [2)] $\Lambda_{\gamma\pi\rho}$ = (0.63 ± 0.11) ef. The spread of the experimental points relative to the theoretical curve with this value of Λ corresponds to χ^2 = 11.09, which lies outside the critical region for the 16% level of significance.

As we have already pointed out at the beginning, the reliability of evaluations of the quantity $\Lambda_{\gamma\pi\rho}$ obtained from data on π^+-meson photoproduction depend to a major extent not only on the accuracy of the experimental results but on the nature of the approximations on which the theoretical calculations are based. The latter fact particularly is responsible in a considerable degree for the contradiction of the different values of the constant Λ reported in the literature.

The opinions given in the literature on the value of $\Lambda_{\gamma\pi\rho}$ can be somewhat arbitrarily broken down into three groups. According to the opinion of one group of authors (for example Höhler and Smidt [19]), comparison of theory with experiment does not indicate the existence of a ρ-meson contribution to

[2)] A similar analysis for six measured angles, excluding 0 and 180°,[18] gave a value of the constant Λ agreeing within experimental error with that obtained using all eight experimental points.

Table II

$a_0^{(4)}$	$a_1^{(4)}$	$a_2^{(4)}$	$a_3^{(4)}$	$a_4^{(4)}$	σ_{tot}
11.98±0.21	—20.93±1.13	9.04±1.31	1.12±1.70	—0.56±1.77	(1.43±0.07)·10^{-28} cm²
0.53±0.01	—0.92±0.05	0.40±0.06	0.05±0.07	—0.02±0.08	2π

The values of $a_i^{(4)}$ are given in units of 10^{-30} cm², and also in units corresponding to a normalization of the total cross section to 2π.

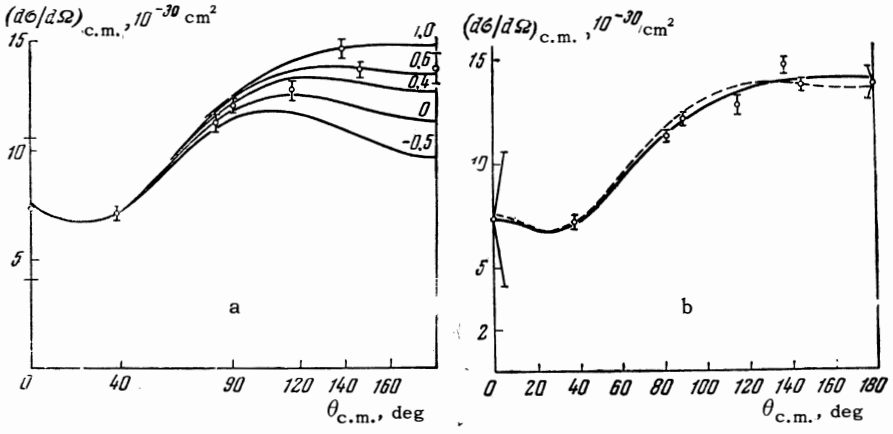

FIG. 10. a – Comparison of the experimental data of the present work with theoretical calculations for different values of the constant $\Lambda_{\gamma\pi\rho}/ef$ (the numbers on the solid curves indicate the values of Λ/ef used in the calculation); b – the solid curve is the approximation of the experimental points by a fourth-degree polynomial in cos $\theta_{c.m.}$. The broken curve is a theoretical calculation for Λ/ef = 0.6.

the pion photoproduction amplitude in the near-threshold region and, thus, $\Lambda_{\gamma\pi\rho} = 0$. According to the opinion of another group, the data existing at the present time support values of $\Lambda_{\gamma\pi\rho}$ in the interval 0—1 (see for example Adamovich et al.[17]). Finally, results have appeared recently on the photoproduction of ρ^0 mesons, from which the width $\Gamma_{\rho\to\pi\gamma}$ has been estimated to be ≈ 1.3 MeV.[20] This estimate was based on use of the single-particle model.[21] The values of the constant (width) given by different authors contain different normalizing factors, which do not always allow direct comparison of the numerical data. Nevertheless, the value of the width $\Gamma_{\rho\to\pi\gamma}$ cited above unconditionally contradicts the value of $\Lambda_{\gamma\pi\rho}$ obtained from photoproduction of single pions, including that of the present work.[3)] The cause of such a discrepancy is not yet clear. It may lie in the failure of the theory to take into account "compensating factors,"[22] which leads to a reduced value of $\Lambda_{\gamma\pi\rho}$ when data on the reaction $\gamma + p \to \pi^+ + n$ are used. However, it is not excluded[23] that the contribution of the single-particle mechanism has been exaggerated in the work of Eisenberg et al.[20].

In addition to determination of $\Lambda_{\gamma\pi\rho}$, the results of the present work have been used to approximate the experimental angular distribution $(1 - \beta \cos\theta_{c.m.})^2 d\sigma/d\Omega_{c.m.}$ by polynomials in powers of cos $\theta_{c.m.}$ The expansion was carried out up to the second, third, fourth, fifth, and sixth powers of cos $\theta_{c.m.}$, inclusively. Unfortunately, the experimental results turned out to be insufficient for a reliable determination of the number of terms of the expansion for which the approximation is best.

The five-term expansion

$$(1 - \beta\cos\theta_{c.m.})^2 \frac{d\sigma}{d\Omega_{c.m.}} = \sum_{i=0}^{4} a_i^{(4)} x^i$$

(where $x = \cos\theta_{c.m.}$) corresponds to inclusion in the π^+-meson photoproduction of S and P waves,[24] which evidently give the main contribution to the process being studied at E_γ = 230 MeV. The values of the regression coefficients $a_i^{(4)}$ obtained in this case are listed in Table II along with the total-cross-section value computed from them. The errors shown for the regression coefficients and the total cross section were obtained on the basis of a combined estimate of the dispersion of the regression curve and of the error matrix.

Figure 10b shows a comparison of the experimental results with the theoretical curve calculated for $\Lambda_{\gamma\pi\rho}/ef = 0.6$[17] and with the regression

3)Meshcheryakov et al.,[27] in their study of the reaction $\pi p \to \pi p\gamma$, separated the contribution of the single-particle diagram by means of the high-energy part of the γ-ray spectrum. As has been shown by Meshcheryakov et al.,[28] the estimate of the width $\Gamma_{\rho\to\pi\gamma}$ which follows from the results of this work should be an order of magnitude less than that obtained by Eisenberg et al.[20].

curve corresponding to a fourth-degree polynomial in cos $\theta_{c.m.}$ (here $\chi^2 = 6.12$).

From the results recently obtained at the Bonn synchrotron on measurement of differential cross sections for photoproduction of π^+ mesons from protons for a wide range of angles and energies,[25] it is evident that the data for $E_\gamma = 230$ MeV and the data of the present work are in good agreement. However, the combination of these two groups of experimental data turns out also to be insufficient for carrying out in complete measure a regression analysis of the angular distribution.

The results listed in Table II, generally speaking, do not have sufficient accuracy for reliable determination of the coupling constant f^2 by the extrapolation method,[26] as follows from analysis of the work of Taylor et al.[26]. The value of coupling constant computed by us

$$f^2 = \left[\sum_{i=0} a_i^{(4)} x^i\right]_{x=1/\beta} \Big/ 20.3 \qquad (2)$$

(the numerical coefficient was obtained from the kinematic characteristics of the photoproduction process and from the universal physical constants) turned out to be equal to $f^2 = 0.07 \pm 0.11$.

In conclusion the authors express their gratitude to P. A. Cerenkov for cooperation in carrying out this work, to A. I. Lebedev for discussion of a number of questions touched upon in the article, to R. A. Latypova and M. S. Kuchumova for formulation of the computer program, and also to A. N. Zinevich and K. I. Yablonin for assistance in the work.

Note added in proof (May 31, 1965). From the report by K. Strauch at the School of Theoretical and Experimental Physics (Erevan, 1965), it follows that the interpretation of Eisenberg's results[20] on the basis of the single-particle mechanism is incorrect, as is correspondingly the value of $\Gamma_{\rho\to\pi\gamma}$ obtained in this work.

[1] Tollestrup, Keck, and Worlock, Phys. Rev. 99, 220 (1955).

[2] Walker, Teasdale, Peterson, and Vette, Phys. Rev. 99, 210 (1955).

[3] Ado, Savel'eva, and Yablokov, PTÉ, 3, 37 (1958), translation: Instruments and Experimental Techniques, 3, 357 (1958).

[4] Aleksandrov, Zinevich, and Leĭkin, Trudy (Proceedings) FIAN 34, (1965), in press.

[5] Dem'yanovskiĭ, Leĭkin, and Yablonin, PTÉ, 3, 82 (1963), translation: Instruments and Experimental Techniques, 3, 452 (1963).

[6] R. R. Wilson, Nucl. Instr. and Methods 1, 101 (1957).

[7] Yu. M. Ado and V. Elyan, FIAN Report R-746, 1961.

[8] V. F. Grushin and A. N. Zinevich, PTÉ, 2, 29 (1958), translation: Instruments and Experimental Techniques, 2, 205 (1958).

[9] V. G. Pol'skiĭ, Dissertation, Moscow Power Institute, 1961.

[10] M. Camac, Rev. Sci. Instr. 22, 197 (1951).

[11] W. Cross, Rev. Sci. Instr. 22, 717 (1951).

[12] M. S. Kozodaev and A. A. Tyapkin, PTÉ, 1, 21 (1956).

[13] Aleksandrov, Grushin, Zapevalov, and Leĭkin, Trudy (Proceedings) FIAN 34, (1965), in press.

[14] R. M. Sternheimer, Phys. Rev. 115, 137 (1959).

[15] W. H. Barkas and S. Von Friesen, Nuovo Cimento 19, Suppl., 41 (1961).

[16] R. M. Sternheimer, Phys. Rev. 124, 2051 (1961).

[17] Adamovich, Larionova, Lebedev, Kharlamov, and Yagudina, Trudy (Proceedings) FIAN 34 (1965), in press.

[18] Aleksandrov, Grushin, Zapevalov, and Leĭkin, DAN SSSR 160, 796 (1965), Soviet Phys. Doklady 10, 131 (1965).

[19] G. Höhler and W. Smidt, Inst. für Theor. Kernphysik, Karlsruhe, preprint, 1963.

[20] Y. Eisenberg et al., Proc. of the Conference on High Energy Physics, Dubna, 1964.

[21] S. Berman and S. Drell, Phys. Rev. 133B, 791 (1964).

[22] A. M. Baldin, Proc. of the Conference on High Energy Physics, Dubna, 1964.

[23] Franklin, Rust, Silverman, Sinclair, and Talman, Phys. Rev. Lett. 13, 491 (1964).

[24] M. Moravcsik, Phys. Rev. 107, 600 (1957).

[25] Freytag, Schwille, and Wedemeyer, Proc. of the Conference on High Energy Physics, Dubna, 1964.

[26] Taylor, Moravcsik, and Uretsky, Phys. Rev. 113, 689 (1959).

[27] Meshcheryakov, Nemenov, and Solov'ev, Proc. of the Conference on High Energy Physics, Dubna, 1964.

[28] Meshcheryakov, Solov'ev, and Tkebuchava, JINR preprint, R-2183, 1965.

Translated by C. S. Robinson
10